AAS 09-128

TIME TAG ISSUES IN THE STAR TRACKER AND GYRO DATA FOR ICESAT PRECISION ATTITUDE DETERMINATION

Sungkoo Bae, Randall Ricklefs,* Noah Smith† and Bob Schutz‡

We describe several time tag problems for ICESat's star trackers and gyros. Problems include star tracker time tag shifts for one or more orbital periods, periodic spikes in the gyro rate, compressed gyro data, and a gyro time tag bias. We discuss possible causes for each problem, the effects on ICESat attitude determination and pointing determination, and methods to handle the problems and meet mission requirements.

INTRODUCTION

The Ice Cloud and land Elevation Satellite (ICESat) was launched on January 13, 2003 into a nearly-circular, frozen orbit, with 94 degrees inclination and an altitude of about 600 km. It was designed to make direct measurements of temporal surface change of the polar ice sheets.[1] The Geoscience Laser Altimeter System (GLAS), which was designed and constructed at NASA Goddard Space Flight Center (GSFC), is carried by ICESat to make these measurements.[2]

GLAS contains three separate Nd:YAG lasers, each of which was designed to operate successively, with a 40 Hz pulse repetition rate. Determining the surface elevation of each laser footprint requires accurate estimation of the spacecraft position, laser pointing direction, and laser travel distance from the spacecraft to the surface spot. Accurate attitude determination enables precise estimation of the laser pointing direction as a unit vector. Precision Attitude Determination (PAD) and Precision Pointing Determination (PPD) processing at the Center for Space Research (CSR) calculate the laser pointing and GLAS optical bench attitude estimates.

PAD/PPD uses Extended Kalman Filter (EKF)[3] processing of data from the Stellar Reference System (SRS)[4] on the GLAS optical bench. The SRS was designed to support accurate attitude determination of the GLAS instrument and the accurate estimate of the laser pointing. It contains two HD-1003 star trackers, Hemispherical Resonator Gyros, a CCD camera to image each transmitted laser pulse at the full 40 Hz rate, a telescope, and associated optics. One of the star trackers, the Instrument Star Tracker (IST), tracks up to six stars in an 8° field of view. Data from the IST and Hemispherical Resonator Gyro (HRG) are processed in the EKF for the optical bench attitude determination. The other star tracker, the Laser Reference Sensor (LRS), is customized to observe a star in a 0.5° field of view, as well as the partial energy of the transmitted laser pulse, at 10 Hz rate. An advantage of the small field of view is that the resolution of the star

* Research Scientist/Engineer, Center for Space Research, University of Texas at Austin, Texas 78712, USA.

† Graduate Student, Center for Space Research, University of Texas at Austin, Texas 78712, USA.

‡ Professor and Associate Director, Center for Space Research, University of Texas at Austin, Texas 78712 USA.

data observed by the LRS is much higher than that from the IST. The high resolution of the LRS was especially helpful in analyzing the gyro time-tag errors discussed in this paper.

The ICESat real-time attitude determination system uses two Ball CT-602 star trackers (BSTs), mounted on the spacecraft bus. The Ball star tracker data is not used directly in PAD processing, but is frequently used for analysis of the PAD results. Each BST tracks up to five stars at 10 Hz rate in an 8° field of view. The two Ball star tracker boresight directions (BD) are nominally 60˚ apart, with the IST BD in the middle. The IST BD is nominally 30˚ from each of the BSTs.

Figure 1 shows a schematic drawing of the spacecraft bus, GLAS, and solar panels. Small circles indicate the relative positions of the star trackers: IST, BST1 and BST2. The spacecraft velocity vector defines two attitude modes: sailboat mode and airplane mode. In airplane mode the spacecraft velocity vector is parallel to the GLAS and bus axis. In sailboat mode the spacecraft velocity vector is perpendicular to the GLAS and bus axis. The sign of the spacecraft velocity vector defines two alternatives for each attitude mode, resulting in four total possibilities. The attitude mode is selected based on solar array requirements and the beta prime angle (the angle between the orbit plane and the sun). Airplane mode is used when the absolute value of beta prime angle is less than 33˚, sailboat mode is used otherwise.

Solar panel motion creates high frequency oscillations in the attitude. The known dominant frequencies are 1.1 and 2.8 Hz. These oscillations have been detected and analyzed using all of the spacecraft attitude sensors, but are clearest in the gyro and LRS data. The oscillations are not present when solar array motion is disabled.

Attitude sensor data transmitted by the spacecraft is assembled by GSFC into GLA04 granules for PAD/PPD processing at CSR. GLA04 granules contain data observed by the SRS, the two Ball star trackers, and flight computer attitude and orbit information. Each data record includes multiple types of time-tags; for example, each gyro record includes time-tag types: UTC, *sample time*, Bus Vehicle Time Code Word (BVTCW) and free-wheeling internal clock time (Table 1). For most records, *sample time* is assigned from the spacecraft clock. IST records are different; the *sample time* is assigned by the IST internal clock. PAD/PPD processing uses GPS seconds based on the *sample time* of each instrument, with an exception that will be discussed later.

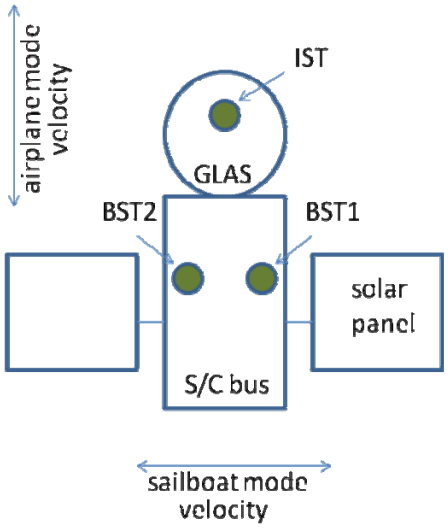

Figure 1. A schematic drawing of the spacecraft bus, GLAS, solar panels and three star trackers. HRGs are located on GLAS, close to the IST.

Table 1. Multiple types of time-tags for gyro data

UTC	sample time	BVTCW	free-wheeling	angle(1,2,3)		
100265386.100343	100265386.128160	100308587.268873	3.573632	1843.70	2487.15	2581.80
100265386.100343	100265386.228494	100308587.369207	3.673600	1830.80	2473.50	2568.75
100265386.100343	100265386.328160	100308587.468873	3.773568	1817.75	2460.90	2555.95
100265386.100343	100265386.428649	100308587.569362	3.873600	1805.00	2448.20	2542.60
100265387.100343	100265386.528185	100308587.668898	3.973632	1792.35	2435.95	2529.25

The mission pointing requirement is a 1σ accuracy of 2 arcseconds in the end-user elevation data products designated as level 428, 429 or 529.[5,6] Various issues had to be addressed in order to achieve this accuracy; several are briefly discussed in Reference 6. The current paper focuses on time tag issues in the IST and HRG data. Incorrect time tagging, regardless of the quality of the measurement in the star tracker and gyros, can cause unacceptable accuracy degradation in PAD/PPD results and in elevation products.

IST TIME-TAG ISSUES

0.1 Second Time-Tag Shift

The boresight direction (BD) is defined as the star tracker z-axis, parallel to the optical axis and perpendicular to the image plane. It can be expressed as the unit vector **u**

$$\mathbf{u} = \boldsymbol{A}^{-1}\ \mathbf{1}_z \tag{1}$$

where $\mathbf{1}_z$ is column vector $[0\ 0\ 1]^T$ and $\boldsymbol{A}^{-1}$ is the inverse of the attitude matrix $\boldsymbol{A}$. The attitude matrix $\boldsymbol{A}$ is estimated by an EKF using star tracker and gyro data. Individual BDs are estimated for the three star trackers: IST, BST1 and BST2.

The angle between the IST BD and BST1 BD (or BST2 BD) is nominally 30˚. In reality the alignments are not exact, can slowly change, and have periodic variations. Variations are caused by bracket motions of the IST and BSTs, as well as relative motion of the GLAS structure and spacecraft bus structure; they are caused by thermal variations over the orbital period. Since the beta prime angle between the sun and orbit plane is changing slowly, by 0.5˚ per day, the orbital variations of the relative attitudes are almost identical from one orbit to the next for a day. The effects of IST bracket motion are discussed in earlier papers.[7,8]

Plots of the computed angles between star tracker BDs are used for verification of PAD/PPD processing. Unexpected jump discontinuities were noticed in plots involving the IST. Figure 2 (a) shows an example of a jump in the computed angle between the IST BD and BST1 BD on day 315 of year 2005. Similar jumps were also found in plots for the IST BD and BST2 BD, but the direction of the jumps was reversed. The day shown in Figure 2 is in the L3d operation period (Oct.-Nov. 2005; the 4th campaign with the 3rd laser) operation period, a sailboat mode campaign. The size of the jump is ~22 arcseconds. Since the ICESat rotation rate around the earth is about ~220 arcseconds per second, and the star trackers are operating at 10 Hz rate, it was suspected that 0.1 second time-tag error existed in either the IST or BST data. There were unexplained gaps in the IST data before and after the angle jumps. The jumps were easily removed by adjusting the IST time-tag by 0.1 second; the result of this correction is shown in Figure 2 (b).

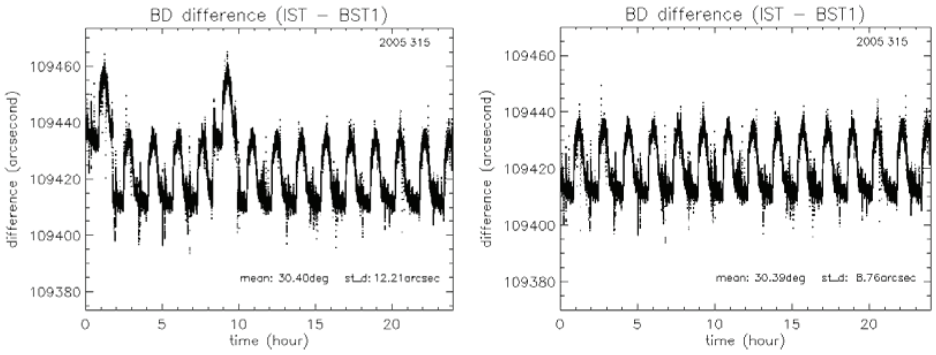

(a) (b)

Figure 2. (a) Jumps in the computed angle between the IST BD and BST1 BD on day 315 of year 2005 (b) Result of the IST time-tag correction by 0.1 second

Adjustment of the BST time-tags would have the same result, but BST 1 and BST 2 did not show any data gaps as in the IST data, and star motion in both BSTs is continuous and normal. We believe that the IST time-tags are erroneously shifted during the initial IST data gap and returned to normal in the following data gap. This empirical adjustment of the IST time-tag is applied before processing.

The L3c campaign (May-June 2005; the 3rd campaign with the 3rd laser) is another example with different characteristics. The angular separations of the boresight directions initially appeared to be normal throughout L3c; jumps were not detected using the method shown above for the L3d campaign. In fact there were jumps, but because L3c was an airplane mode campaign a different method was needed to detect them than the method used above for the sailboat mode L3d campaign. The problem was initially detected in the elevation products. ICESat elevations during the L3c campaign showed anomalies when validated using ocean data analysis; daily mean values of about half of the 33 campaign days were not in the expected range. Ocean data analysis is one method for calibration and validation of the ICESat elevation products; ICESat elevations over the ocean are compared to elevations from mean sea surface.[9] One of the parameters regularly compared is the daily mean of the elevation difference.

Figure 3 (a) shows the first component of the quaternion difference between the IST and BST1 for L3c campaign day 154 of year 2005. Similar jumps in the quaternion difference were also found at the time of the L3d jumps in Figure 2 (a). The reason the L3c BD angle did not show variations can be explained with the geometry of the star tracker BDs with respect to the ICESat velocity vector as shown in Figure 4. In airplane mode the BD angle is not sensitive to the time tag shift because the velocity vector is perpendicular to the plane of the star tracker boresights. In sailboat mode the BD angle is sensitive to the time-tag shift because the velocity vector is in the same plane as the star tracker boresights. In sailboat mode, if one of the star trackers has a time-tag error the BD angle is affected proportionally to the spacecraft rotation rate of ~220 arcseconds per second. Differencing the star tracker attitude quaternions reveals any time-tag shift regardless of the attitude mode.

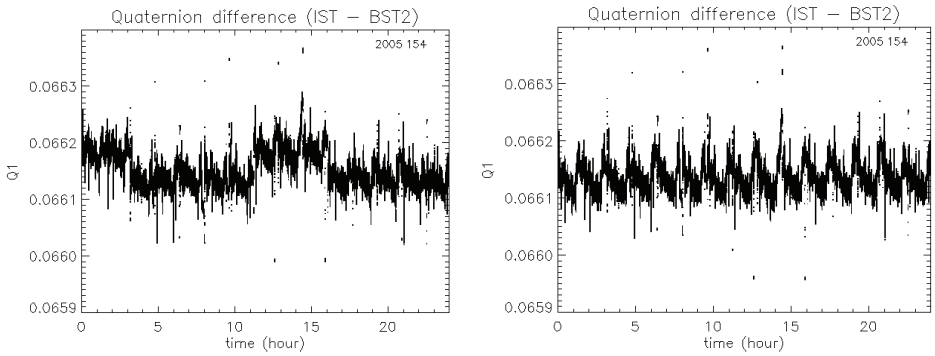

(a) (b)

Figure 3. (a) Jumps in the first component of the quaternion difference between the IST and BST1 for day 154 of year 2005 (b) Result of the IST time-tag correction by 0.1 second

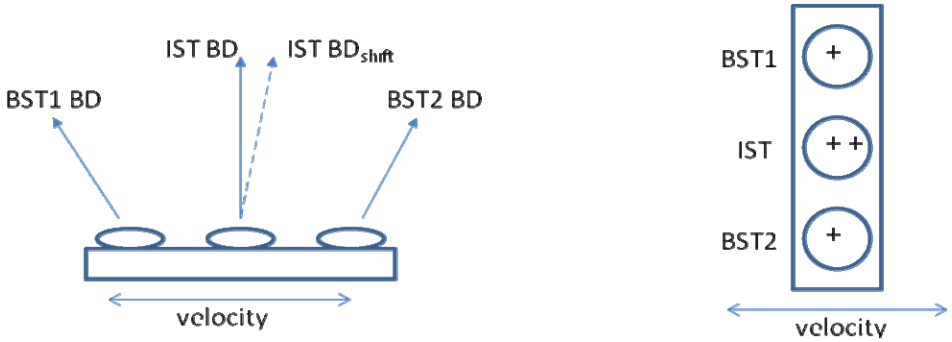

(a) (b)

Figure 4. Geometry of the star tracker BDs with respect to the ICESat velocity vector (a) sailboat mode (b) airplane mode

Time-tag shifts always begin and end during data gaps. During airplane mode the sun is close to the IST BD and periodic sun-blinding causes data gaps of several hundred seconds; time-tag shifts begin and ends during these gaps. The large number of airplane mode sun-blinding data-gaps correlate with the large number of time-tag shifts.

The source of the IST time-tag shift is not yet known. One possibility is that it is introduced during ground processing. In order to check this, we examine the motion of a star observed simultaneously by the IST and LRS. Figure 5 shows a component of the quaternion difference for day 146 of year 2005. The differenced quaternions were obtained from IST and BST2 data by using the QUEST method.[10] The QUEST method does not use gyro data. Arrows in Figure 5 indicate times when IST star 11482 was observed simultaneously by both the IST and LRS.

Table 2 shows time and position differences between the IST and LRS measurements of star 11482 at the labeled positions S_0, S_1,S_2,S_3 and S_4. The measurement time differences, t_{ist}-$t_{lrs,}$ are less than 10 milliseconds. The star was moving parallel to the *y*-axis in both IST and LRS. Because the resolutions of IST and LRS are not the same, the difference of *y* coordinates of the

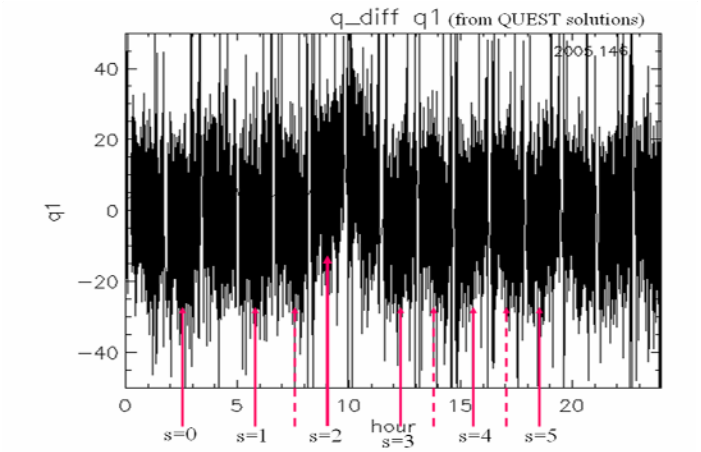

Figure 5. A component of the QUEST quaternion difference for day 146 of year 2005. Measurement time of the commonly observed star (IST star catalog number 11482) by the IST and LRS is indicated by arrows.

star, Δy_{exp}, should change between consecutively labeled positions by constant amount; about 5.57 arcseconds. Actual difference of *y* coordinates, Δy_{obs} (5^{th} column), was compared to expected difference, Δy_{exp} (6^{th} column), and the result, Δy_{obs}-Δy_{exp}, is shown in the last column. Unusual 21.69 arcseconds difference between the expected and the observed is obvious at measurement point S_2, where the abnormal jumps occurred in Figure 5. It proves the time-tag shift in the IST data by 0.1 second.

The search for the exact starting point of IST time-tag shifts has not been successful due to the complicated time-tag system and other anomalies in the IST data such as frequent 0.1 second time-tag skips that will be discussed in the next section. In addition the 0.1 second time-tag shift always happens when the star data is not available.

Using the quaternion difference plots like the one in Figure 3 (a), the approximate starting and ending times of the IST time-tag 0.1 second shift were determined. Time-tags were empirically corrected whenever the quaternion difference jumps were occurred. Corrected IST data does not show jumps of the quaternion difference as shown in Figure 3 (b).

Table 2. Time and position differences between the IST and LRS measurements of star 11482 at the labeled positions in Figure 5

S	t_{ist}	t_{ist}-t_{lrs}	x_{ist}-x_{lrs}	y_{ist}-y_{lrs} (Δy_{obs})	606.84-5.57*S (Δy_{exp})	Δy_{obs}-Δy_{exp}
0	9292.155	0.004	1389.23	606.84	606.84	0.00
1	20892.153	0.002	1396.68	599.45	601.27	-1.82
2	32492.151	-0.001	1397.84	617.39	595.70	**21.69**
3	44092.149	-0.003	1400.47	588.63	590.13	-1.50
4	55692.147	-0.006	1405.08	584.55	584.56	-0.01

Time Reversals, Data Duplicates and Data Skips

Early in the mission IST time reversals and data duplicates impeded the PAD processing or caused large errors in the attitude estimates. In a time reversal the data time-tags are not in increasing order. In a data duplicate the data is the same at successive time-tags. In a data skip, there is at least 0.1 second data gap between the successive IST data record. These problems were unexpected before the real data was available. The time tag problem was usually first detected by an abnormal interruption in the PAD processing or large uncertainties in the attitude solution. The comparison between different solutions, EKF vs QUEST or IST vs BST, sometimes showed strange results that could not be reasonably explained.

The source of the problem that caused the time-tag errors was the time to center of integration (COI) in the downlinked data from the spacecraft. The IST data has its own internal time-tag (sample time) at 10 Hz rate for every star tracker frame. The COI is also recorded at 10Hz rate. It is added to the IST time-tag to form the time of the closest shot. The 1Hz UTC time is used with the COI corrected IST time-tag to produce the 10Hz UTC time. Originally the COI number was expected to be about 50 milliseconds. It turns out the actual COI is frequently bigger than the expected number and drifts, sometimes with unreasonably large jumps. The addition of the bad COI to the IST time-tag resulted in various time-tag issues. A joint effort by the GSFC and CSR attacked these issues and eventually removed or greatly reduced the impact on the pointing determination.

GYRO TIME-TAG ISSUES

Periodic HRG Rate Spike

At the beginning of the mission, the time-tag of the gyro data for the PAD was based on the *sample time* in the GLA04 data. Unusual peaks were found every ~220 seconds in pitch rate of the gyro data (Figure. 6 (a)). To study the cause of these peaks, the angular rate was independently derived from the QUEST solution of the star tracker data.

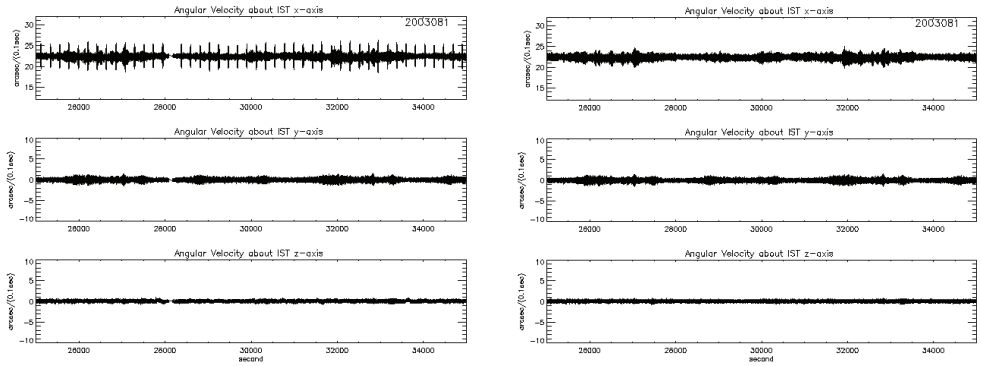

(a) (b)

Figure 6. (a) Gyro rates in three IST axes when the *sample time* was used on day 81 of year 2003 (b) Gyro rates in three IST axes when the SIRU time-tag was used

The rate derived from the QUEST solution did not show those peaks, so the source of the peaks seemed to be an unknown systematic error in the gyro data. Looking into various time-tags associated with the gyro data, the periodic peaks seemed to be caused by the difference between the two clock times: the time recorded by gyro's free-wheeling internal clock (SIRU clock) and the external *sample time* associated with the spacecraft clock.

The gyro *sample time* is closely related to the VTCW that is acquired from the spacecraft clock. Figure 7 shows the relationship between the *sample time* and the VTCW. The difference of two time-tags is negligible in our application. Since the spacecraft clock provides a link to absolute time, the *sample time* seems to be the logical choice for the gyro data for use in the attitude determination. The SIRU clock, internal to the SIRU, latches the gyro values and time-tags once every 10 milliseconds, but the spacecraft system acquires one of these sets once every 100 milliseconds. The *sample time* is designed to be assigned to the gyro angle within the 10 milliseconds difference range from the SIRU time-tag.

Sample time has a constant 10 Hz rate. The SIRU time-tags vary from 10 Hz rate; there are periods when the nominal 0.1 second interval changes to the sequence 0.09, 0.1 and 0.11 seconds. This sequence repeats for about 20 seconds and then occurs again after about 220 seconds. Since the SIRU clock latches data at 100Hz these 10 millisecond interval variations may be related to the random behavior of the SIRU frequency. If *sample time* is used, then gyro rate peaks appear during the periods of varying SIRU time-tag rate. There are no gyro rate peaks when the SIRU time-tags are used (Figure 6 (b)).

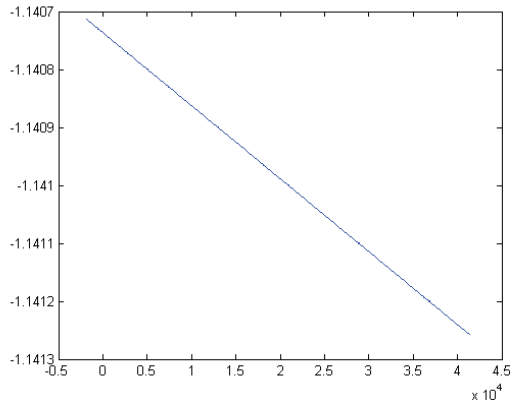

Figure 7. *Sample time* – VTCW for day 65 of year 2003 shows ~1 millisecond change over a day

Compressed Gyro Data

Switching from *sample time* to SIRU time-tags caused the EKF attitude solution to drift relative to the QUEST solution (Figure 8 (a)); there is no drift when *sample time* is used. Investigation lead to the conclusion that the use of the SIRU time-tags cause the data time span compressed: 24 hours of gyro data is recorded in the time length that is several seconds shorter than actual 24 hours.

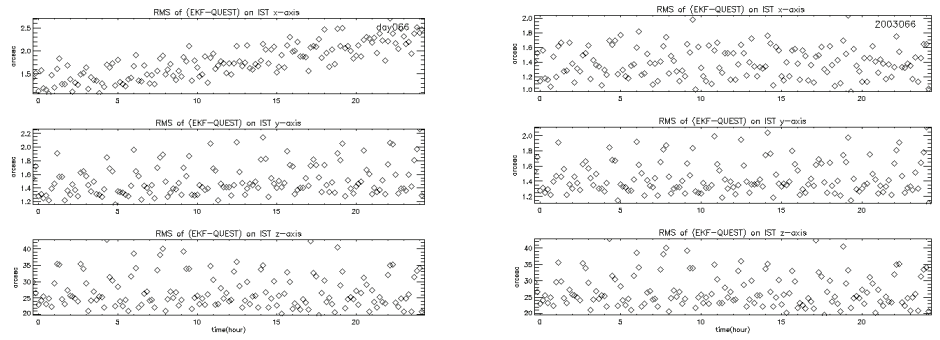

(a) (b)

Figure 8. (a) Drift of EKF attitude with respect to QUEST attitude due to compressed gyro time-tags for day 66 of year 2003. (b) No more drift of EKF attitude after gyro time-tag stretch.

The SIRU clock has different rate from the spacecraft clock. The SIRU and *sample time* time-tags are recorded together in 10Hz records as determined by the spacecraft clock (see Table 1). Occasionally a SIRU time-tag is not included with the sample time in a record because the rate of the SIRU clock is generally faster than the rate of the spacecraft clock. Using *sample time* avoids the time skip, but it causes the problem discussed in the previous section.

Each 0.1 second SIRU time-tag skip was corrected by subtracting 0.1 second to make the gyro data continuous. Normal processing is for one day of data; the start and end of the day are based on the spacecraft clock *sample time*. All 0.1 second subtractions from the SIRU time-tag accumulate throughout the day; at the end of the day, the corrected SIRU time-tags have not reached 86400 seconds. As an example, the corrected SIRU time-tags for day 66 of year 2003 reached 86396 seconds. The SIRU time-tags are effectively compressed in time. The cumulative effect of the SIRU time-tag compression becomes noticeable about 6 hours after the start of the day as shown in Figure 8 (a).

To stretch the compressed time-tags to 24 hours, a scale factor (*sf*) between the *sample time* and SIRU time-tag is computed

$$sf = 86400 / \text{ length of day for the compressed SIRU time-tags}$$

For example, the *sf* for day 66 of year 2003 is

$$sf = 86400 / 86395 = 1.0000578737$$

The stretched SIRU time-tag, t_{str}, is computed by

$$t_{str} = t_{comp,0} + (t_{comp} - t_{,comp,0}) * sf$$

where t_{comp} is the SIRU time-tag and $t_{comp,0}$ is the initial SIRU time-tag of the day; the effect of this correction is shown in Figure 8 (b).

The amount of SIRU time-tag compression varies with the optical bench temperature so the scale factor is not a constant value. Large scale factor variations have occurred at major spacecraft thermal events; the scale factor is adjusted daily. Another solution for data skips in the SIRU time-tags is to use interpolated gyro rates with IST time-tag; however, stretched SIRU time-tags have performed well.

Constant Bias

ICESat surface elevations over a flat Bolivian salt lake contained a 2.8 Hz oscillation. It was an indication that the PAD/PPD did not properly handle the known spacecraft oscillation that originated from the solar array articulation.

High resolution measurements of star motion by the LRS were useful for analyzing the 2.8 Hz oscillation. Star motion in the LRS *x* and *y* axes was transformed into a two axis rotation of the spacecraft; this rotation was also estimated using the gyros. A comparison of the spacecraft rotation estimated using both LRS star motion and gyros is shown in Figure 9. The gyro curve is offset by about 50 milliseconds in time from the LRS curve; when PAD/PPD was done with this 50 millisecond offset removed from the gyro time-tags, the 2.8 Hz oscillation in the ICESat surface elevations vanished.

Figure 10 shows the average gyro time-tag offset for each laser operation period (L1 to L3j, i.e., 2003 to 2008), determined by comparing the spacecraft rotation estimated using both LRS star motion and gyros. A 50 millisecond bias was removed from the gyro time-tags before the comparison. The mean gyro time-tag offset is 6.8 milliseconds. There is no evidence that these offsets are entirely in the gyro time-tags; the LRS time-tag could also be shifted from absolute time by several milliseconds.

Comparisons were also made of the spacecraft rotation estimated using LRS star motion and star motion in the other star trackers; the time-tags of the star trackers were also compared to the LRS star motion for L3i (Oct.-Nov. 2007) and L3j (Feb.-Mar. 2007) campaigns, the most recent campaigns at the time of investigation. Star position uncertainty for the star trackers is relatively high compared to the LRS, and does not provide good resolution for comparison. Instead of individual star motions, the star tracker EKF quaternion was used in the analysis. The attitude rates, computed from the quaternion, are integrated to the angles.

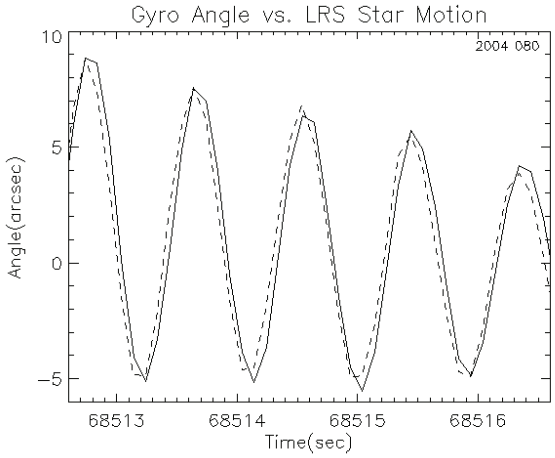

Figure 9. Gyro angle (sold line) is offset by about 50 milliseconds in time from LRS star motion (dotted line) on day 80 of year 2004.

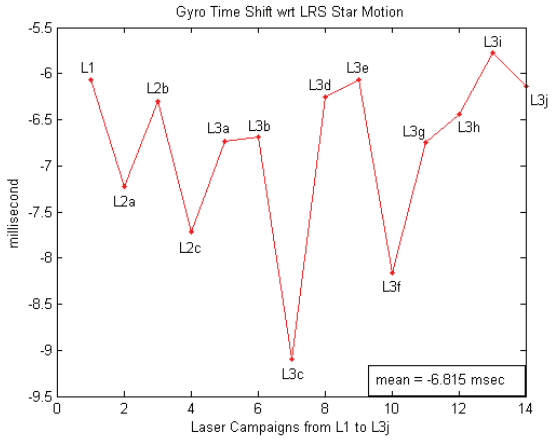

Figure 10. Motions of all LRS stars in each campaign are compared with gyro angle to compute the mean time-tag offset. Airplane mode campaigns (L2c, L3c and L3f) show relatively larger offsets than sailboat mode campaigns.

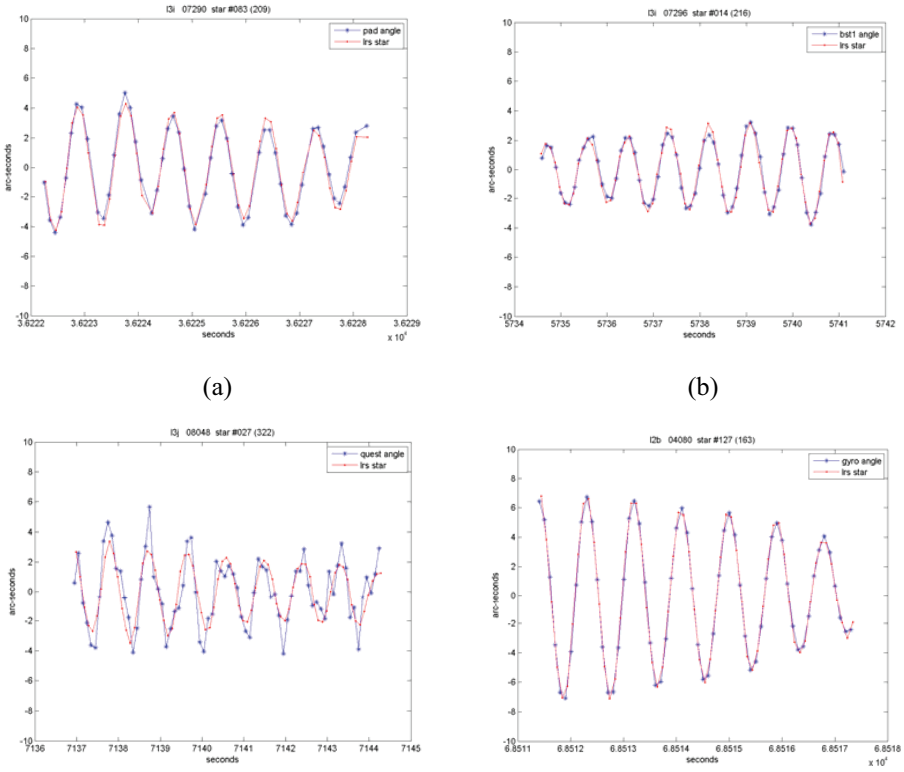

(a) (b)

(c) (d)

Figure 11. Comparison examples, after ~50 millisecond gyro time-tag shift, between LRS star motion and angle from (a) IST EKF quaternion (b) BST1 EKF quaternion (c) IST QUEST quaternion (d) gyro data

Figure 11 in the previous page shows comparisons between LRS star motion and star tracker attitude angles after 50 millisecond gyro time-tag adjustment. Figures 11 (a) and 11 (b) compare LRS star motion with IST and BST1. Gyro data is included by the EKF. In order to exclude gyro effects, the QUEST quaternion was used instead of the EKF quaternion in Figure 11 (c). This particular example shows relatively good comparison of the spacecraft rotation estimated using the IST and LRS star motion. However, the QUEST quaternion is, most of time, too noisy to compute the time-tag offset against the LRS star motion. Figure 11 (d) shows a comparison of the spacecraft rotation estimated using both LRS star motion and gyros by using the same data for Figure 9.

For all laser campaigns a 50 millisecond correction was applied to gyro data. The effect of any remaining bias of the gyro time-tag is negligible for the elevation product. Table 3 shows the time-tag offset between all three star tracker solutions and LRS star motion in millisecond unit for L3i and L3j campaigns. For comparison, gyro time-tag offset is also given in the table. There are no tens of milliseconds level differences.

Table 3. Mean time-tag offsets between LRS star motion and EKF quaternions from three star tracker measurements in millisecond unit for L3i and L3j campaigns

	L3i	L3j
IST	-2.6	-3.2
BST1	-4.2	-5.3
BST2	-4.3	-4.5
GYRO	-5.8	-6.2

INSTRUMENT SAMPLE RATE DIFFERENCES

The nominal sample rate of the star trackers and gyros is 10 Hz; however, time-tags show that each instrument has a unique rate. The Ball star trackers and LRS time-tags are relatively near 10 Hz, IST time-tags show a slower rate, and the gyro time-tags a faster rate. Figure 12 shows the difference of the IST and gyro time-tags; the difference varies linearly with time. The difference in time-tag rates can introduce errors if it is not properly handled. For ICESat PAD, IST data has the highest priority and non-IST time-tags are interpolated to match IST time-tags.

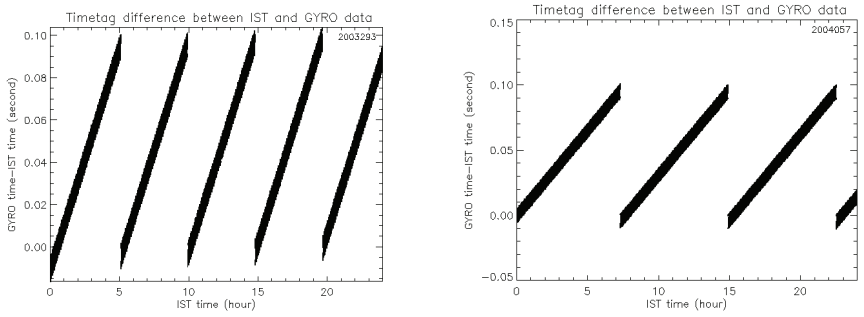

Figure 12. Time-tag differences between IST and HRG data on day 293 of year 2003 and day 57 of year 2004. IST clock has slower rate than SIRU clock.

CONCLUSION

In the raw IST data, the time to Center of Integration (COI) was not in the expected range and caused time-tag reversals, skips and data duplicates. The source of the occasional 0.1 second shift during the long data gaps is not yet known. The tri-modal pattern of the SIRU time-tag interval created periodic peaks in the gyro rate when the time-tag based on the spacecraft clock was used. Peaks were removed by using the SIRU time-tag, but the faster rate of the SIRU clock compared to the spacecraft clock caused the EKF solution to drift. The EKF attitude solution had an error due to the gyro time-tag bias of ~50 milliseconds. Different rates of different sensors' clocks can be the source of attitude error if not handled properly.

In the development of the PAD algorithms and software before the ICESat launch, the star positions and gyro angles were given much more attention than the time-tags that accompanied them. Soon after the start of processing real flight data, time-tag problems became major issues. Because of the demanding mission PAD/PPD requirement, 1σ of 2 arcseconds, the time-tag errors, whether systematic or random, were the source of the unacceptable attitude/pointing error.

Some of these problems could be common to any missions that use star trackers and gyros, but some might be unique to the ICESat PAD. All problems have been resolved adequately, in some cases with considerable effort. The cause of each problem, the influence on the ICESat PAD, and the method of handling needed to meet the mission PAD requirement were discussed. Further research is still required to understand the source for the occasional 0.1 second IST time-tag shift. Knowing the possible time-tag issues in the star tracker and gyro would help to prepare better algorithm and software for future missions.

ACKNOWLEDGMENTS

The authors are grateful to David Hancock at GSFC and Marcos Sirota at Sigma Space Corp for valuable information and discussions about the ICESat time-tag system design. Special thanks to Sungpil Yoon for the work in the PAD/PPD processing and analysis. The work was supported by NASA ICESat.

REFERENCES

[1] J. Zwally, et al., "ICESat's laser measurements of polar ice, atmosphere, ocean and land", *J.Geodyn*., V.34, 405-445, 2002.

[2] J. Abshire, et al., "Geoscience Laser Altimeter System (GLAS) on the ICESat mission: on-orbit measurement performance", *Geophys. Res. Letter*, Vol 32, L21S02, doi:10.1029/2005GL024028, 2005.

[3] E.F. Lefferts, F.L. Markley, and M.D. Shuster, "Kalman filterming for spacecraft attitude estimation", *J. Guidance, Control, and Dynamics*, 5(5), 417-429, 1982.

[4] M. Sirota, et al., "The transmitter pointing determination in the Geoscience Laser Altimeter System", *Geophys. Res. Letters*, V. 32, L22S11, doi:10.1029/2005GL024005, 2005.

[5] L. Magruder, E. Silverberg, C. Webb, and B. Schutz, "Pointing and timing validation of the ICESat laser altimeter", *IEEE Trans. in Geoscience and Remote Sensing*, Vol. 45, No. 1, 147-155, Jan. 2007.

[6] B. Schutz, S. Bae, N. Smith, and M. Sirota, "Precision Orbit and Attitude Determination for ICESat", F. Landis Markley Astronautics Symposium, Paper AAS 08-305, Cambridge, MD. Jun.29-Jul.2, 2008.

[7] S. Bae, C. Webb and B. Schutz, "GLAS PAD calibration using Laser Reference Sensor Data", AIAA/AAS Astrodynamics Specialist Conference, Paper AIAA 2004-4857, Aug. 2004.

[8] S. Bae, and B. Schutz, "Precision attitude determination using gyro and star tracker data with a batch least-squares estimator", *Advances In the Astronautical Sciences*, Vol. 123, 175-182, Univelt Publishing, 2006.

[9] T. Urban, and B. Schutz, "ICESat sea level comparisons", *Geophys. Res. Lett.*, 32, L23S10, doi:10.1029/2005 GL024306, 2005.

[10] M. Shuster, and S. Oh, "Three-axis attitude determination from vector observations", *J. Guidance, Control, and Dynamics*, 4(1), 70-77, 1981.